

Supplementary Information

Lignin organic-inorganic supramolecular aggregates derived N, O co-doped porous carbon nanosheets for high performance zinc-ion hybrid capacitors

*Yukang Fan,^a Dongjie Yang,^{a, *} Fangbao Fu,^b Xueqing Qiu^{b, *} and Wenli Zhang^b*

^a School of Chemistry and Chemical Engineering, Guangdong Provincial Key Laboratory of Green Chemical Product Technology, Guangdong Provincial Key Laboratory of Fuel Cell Technology, South China University of Technology, Guangzhou, 510641, China

^b School of Chemical Engineering and Light Industry, Guangdong University of Technology, Guangzhou, 510006, China

* E-mail address for the Corresponding author: cedjyang@scut.edu.cn (D. Yang), cexqiu@scut.edu.cn (X. Qiu).

1. Characterizations

The micromorphology of the samples was acquired using scanning electron microscopy (SEM, Hitachi SU8220) at 10 kV and field emission transmission electron microscopy (TEM, JEM 2100F) at 200 kV. The characteristic functional groups of the samples were characterized by Attenuated Total Reflection Fourier Transform Infrared Spectroscopy (ATR-FTIR, Thermo Scientific Nicolet iS50). The chemical composition and phase analysis of the samples were performed using Raman spectroscopy (Raman, HJY LabRAM Aramis), X-ray diffraction (XRD, Bruker D8 Advance), and X-ray photoelectron spectroscopy (XPS, Thermo Scientific KAlpha). The N₂ adsorption-desorption isotherms of carbons were determined using an Automatic surface and porosity analyzer (Micromeritics ASAP 2460) at a temperature of 77 K. The pore size distribution was calculated using the Density Functional Theory (DFT) model, and the specific surface area was determined through the Brunauer-Emmett-Teller (BET) method. The thermal decomposition behavior of the precursor was examined in a N₂ atmosphere with the assistance of a thermal analyzer (TGA, TA TGA55) and a thermal gravimetric-infrared technique (TG-FTIR, Thermo Scientific Nicolet iS50). The static contact angle of electrolyte drop on the surface of the electrode material was recorded using a static contact angle measuring instrument (SINDIN, SDC-350).

2. Electrochemical Performance Measurements

The working electrodes were prepared by mixing 80 wt.% active material, 10 wt.% acetylene black, and 10 wt.% a dispersed PTFE solution, which was then ground in an ethanol solution until homogeneous. Subsequently, the mixture was rolled into a working electrode with a loading of 1.5-2.0 mg/cm². The dried electrode was pressed onto a stainless-steel current collector at a pressure of 10 MPa to obtain a working electrode with an area of approximately 1.0 cm². Finally, the Zn-ion hybrid

capacitors (ZIHCS) were assembled using as-prepared carbon materials as the cathode, zinc foil as the anode (pre-polished and ground to eliminate the surface oxide layer), 100 μL of 1 M ZnSO_4 as the electrolyte, and the glass fibers (Whatman GF/D) as the separator.

The constant current charge-discharge (GCD) curves, cyclic voltammetry (CV) curves, electrochemical impedance spectroscopy (EIS), and self-discharge tests were conducted using an electrochemical workstation (VMP3e, Biologic). The cycling performance was evaluated using the Neware battery test system. EIS spectra were measured by three-electrode system testing in the frequency range of 1000 kHz to 10 mHz with a voltage amplitude of 5 mV. All electrochemical tests were performed at room temperature, with a voltage window ranging from 0.2 to 1.8 V.

The specific capacitance (C_g , F/g) of the electrode material based on the ZIHCS was calculated from the discharge curve of the GCD by the following equation:

$$C_g = I \Delta t / m \Delta V \quad (1)$$

Where I (A) and Δt (s) are the charging/discharging current and discharge time, while m (g) is the mass of the active materials, and ΔV (V) is the voltage change during the discharge time Δt .

The energy density (E_g , Wh/kg) and power density (P_g , W/kg) of the ZIHCS were calculated by the following equations:

$$E_g = C_g \times \Delta V^2 / (2 \times 3.6) \quad (2)$$

$$P_g = E_g \times 3600 / \Delta t \quad (3)$$

where C_g (F/g) is the specific capacitance calculated from the discharge curve based on the ZHSCs, ΔV (V) is the potential window, and Δt (s) is the discharge time.

The real capacitances (C'), imaginary capacitances (C'') and relaxation time (τ) based on EIS measurement to evaluate the capacitance response speed, were calculated using the following

equations:

$$C' = -Z'' / (2\pi f A |Z|^2) \quad (4)$$

$$C'' = Z' / (2\pi f A |Z|^2) \quad (5)$$

$$\tau = 1/f_0 \quad (6)$$

where Z'' is the imaginary impedance, Z' is the real impedance, f is the frequency, A is available surface area, and $|Z|$ is the magnitude of impedance. f_0 is the frequency at which the C'' reaches the maximum.

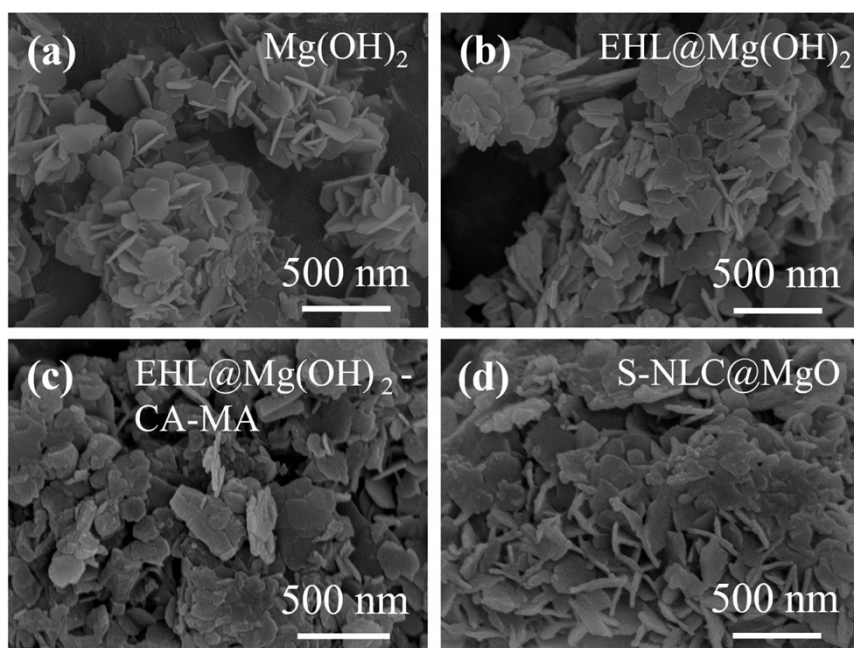


Figure S1 SEM images of $\text{Mg}(\text{OH})_2$ (a), $\text{EHL@Mg}(\text{OH})_2$ (b), $\text{EHL@Mg}(\text{OH})_2\text{-CA-MA}$ (c), and S-NLC@MgO (d).

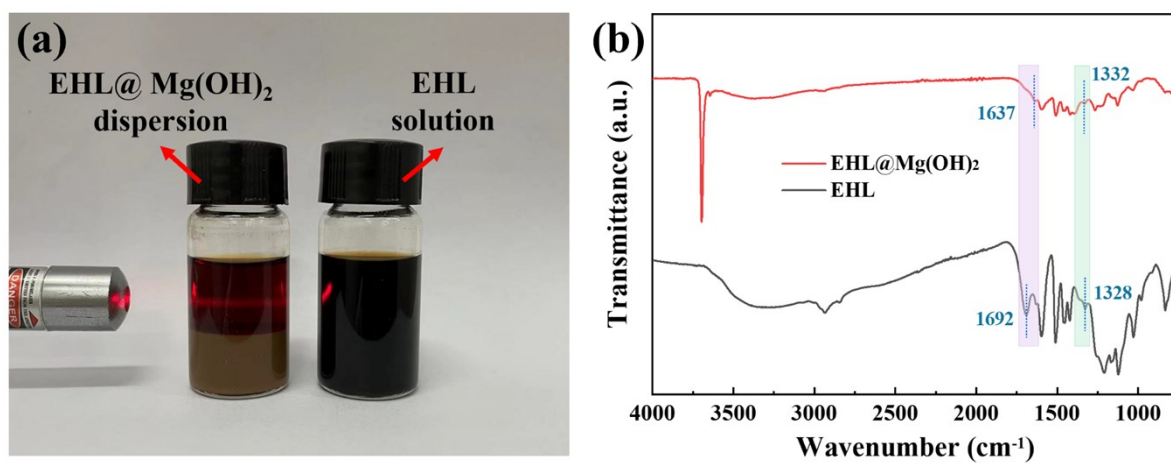


Figure S2 (a) Digital photograph of the red beam through the $\text{EHL@Mg}(\text{OH})_2$ dispersion (left) and the EHL solution (right). (b) The FTIR spectra of EHL and $\text{EHL@Mg}(\text{OH})_2$.

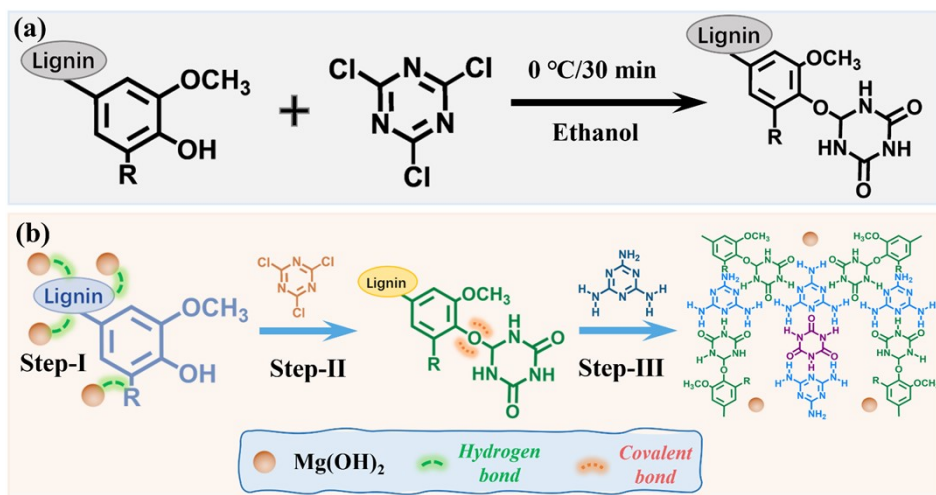


Figure S3 (a) The cross-linking reaction between EHL and cyanuric trioxide. (b) Schematic diagram of the formation process of lignin-based organic-inorganic supramolecular aggregates.

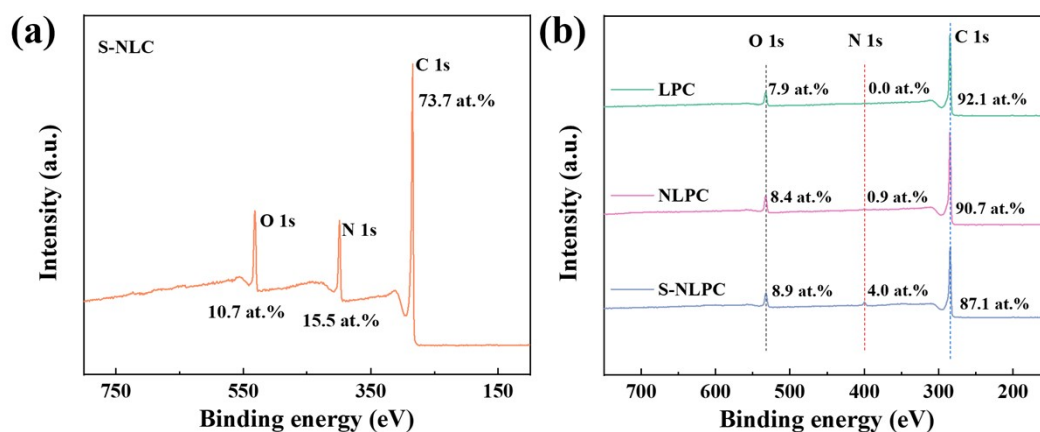


Figure S4 (a) XPS survey spectra of S-NLC. (b) XPS survey spectra of LPC, NLPC, and S-NLPC.

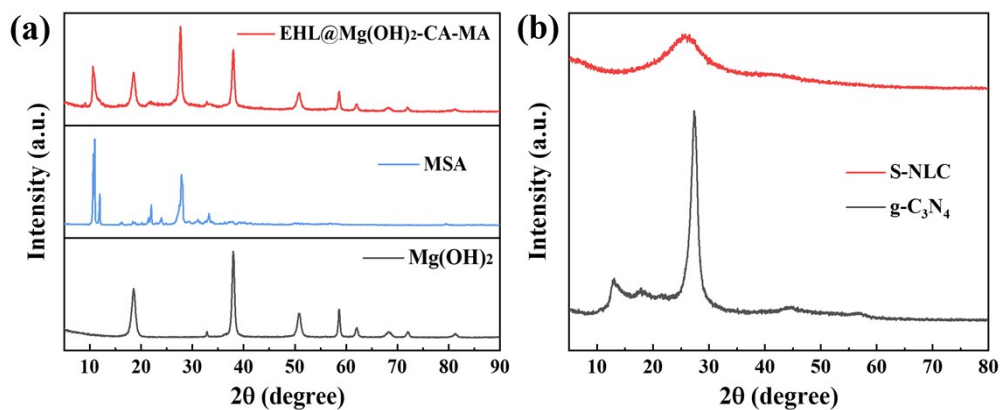


Figure S5 (a) XRD patterns of EHL@Mg(OH)₂-CA-MA, MSA and Mg(OH)₂. (b) XRD patterns of S-NLC and g-C₃N₄.

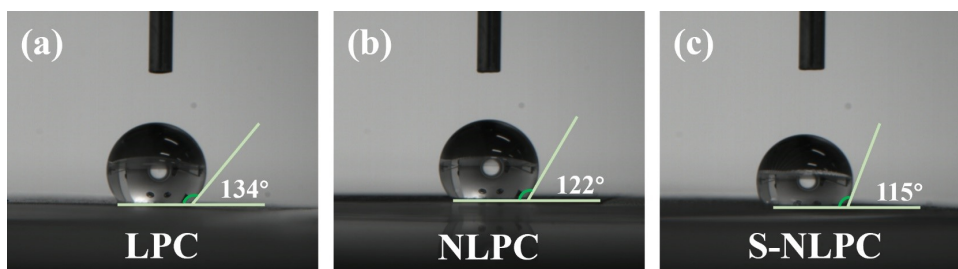


Figure S6 The electrolyte contact angle for LPC (a), NLPC (b), S-NLPC (c).

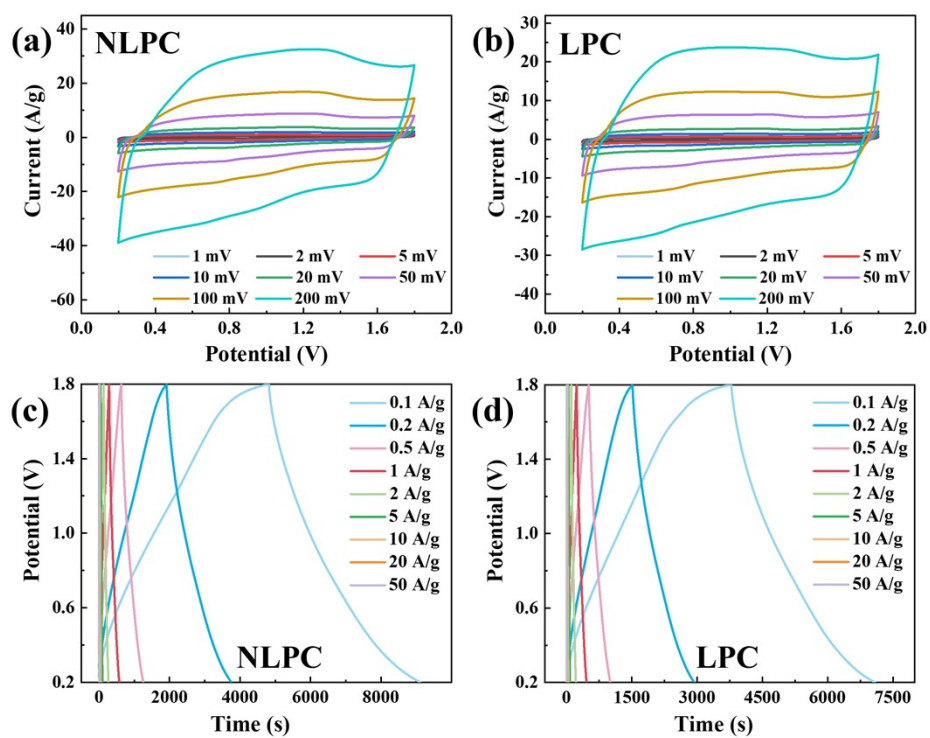


Figure S7 CV curves of NLPC (a) and LPC (b). GCD curves of NLPC (c) and LPC (d).

Table S1 Comparison of the electrochemical performance of ZIHCs based on S-NLPC cathode with reported literature

Precursors	Materials	SSA (m ² /g)	Test conditions	C (F/g)	Refs
Graphene	rGO-200	-	1 M ZnSO ₄ 0.5 A/g	245.0	1
Graphene	P-CNT/rGO	236.7	2 M ZnSO ₄ 0.5 A/g	213.4	2
Graphene	GMF-G@RuO ₂	1190.9	2 M ZnSO ₄ 0.1A/g	170.4	3
Graphene	NB-CQDs/rGO	447.9	2 M ZnSO ₄ 0.2 A/g	261.3	4
Graphene	EG-RGO	216.3	1 M ZnSO ₄ 0.1 A/g	327.4	5
MOFs	MPC-2	2125.0	3 M Zn(CF ₃ SO ₃) ₂ 0.2 A/g	289.2	6
Biomass	OLDC-750	2259.5	2 M ZnSO ₄ 0.1 A/g	306.8	7
Biomass	SMC-800	686.3	2 M ZnSO ₄ 0.1 A/g	313.01	8
Lignin	LPC-600	860.5	1 M ZnSO ₄ 0.1 A/g	178.0	9
Lignin	L-N-CNS	643.9	1 M ZnSO ₄ 0.1 A/g	233.4	10
Lignin	LNPC-800	657.0	1 M ZnSO ₄ 0.05 A/g	266.0	11
Lignin	AL-KNPC-800	1949.0	1 M ZnSO ₄ 0.1 A/g	360	12
Biomass	S-NLPC	2848.1	1 M ZnSO ₄ 0.1 A/g	433	This work

SSA: Specific surface area, C: Specific capacitance

References

1. H. Xu, W. He, Z. Li, J. Chi, J. Jiang, K. Huang, S. Li, G. Sun, H. Dou and X. Zhang, *Adv. Funct. Mater.*, 2022, **32**, 2111131.
2. J. Yao, F. Li, R. Zhou, C. Guo, X. Liu and Y. Zhu, *Chin. Chem. Lett.*, 2024, **35**, 108354.
3. Y. Yu, P. Yang, R. Yan, F. Ren, S. Yu, L. Zhang, J. Guo, R. Li and J. Xie, *J. Energy Storage*, 2024, **80**, 110368.
4. J. Yao, C. Liu, J. Li, Z. Hu, R. Zhou, C. Guo, X. Liu, F. Yang and Y. Zhu, *Rare Met.*, 2023, **42**, 2307-2323.
5. H. Jiang, Y. Zhang, F. Sheng, W. Li, J. Li, D. Huang, P. Guo, Y. Wang and H. Zhu, *ACS Appl. Mater. Interfaces*, 2023, **15**, 13086-13096.
6. H. Li, J. Wu, L. Wang, Q. Liao, X. Niu, D. Zhang and K. Wang, *Chem. Eng. J.*, 2022, **428**, 131071.
7. H. Li, P. Su, Q. Liao, Y. Liu, Y. Li, X. Niu, X. Liu and K. Wang, *Small*, 2023, **19**, 2304172.
8. A. Samage, M. Halakarni, H. Yoon and N. Sanna Kotrappanavar, *Carbon*, 2023, **219**, 118774.
9. J. Zhu, T. Huang, M. Lu, X. Qiu and W. Zhang, *Green Chem.*, 2024, **26**, 5441-5451.
10. W. Jian, W. Zhang, X. Wei, B. Wu, W. Liang, Y. Wu, J. Yin, K. Lu, Y. Chen, H. N. Alshareef and X. Qiu, *Adv. Funct. Mater.*, 2022, **32**, 2209914.
11. W. Zhang, J. Yin, W. Jian, Y. Wu, L. Chen, M. Sun, U. Schwingenschlögl, X. Qiu and H. N. Alshareef, *Nano Energy*, 2022, **103**, 107827.
12. B. Xue, C. Liu, X. Wang, Y. Feng, J. Xu, F. Gong and R. Xiao, *Chem. Eng. J.*, 2024, **480**, 147994.